Crystal Structure of Superconducting $K_3Ba_3C_{60}$: A Combined Synchrotron X-ray and Neutron Diffraction Study

Serena Margadonna, Efstathios Aslanis, Wen Zhi Li, and Kosmas Prassides*

Fullerene Science Centre, School of Chemistry, Physics and Environmental Science, University of Sussex, Brighton BN1 9QJ, UK

Andrew N. Fitch

European Synchrotron Radiation Facility, B. P. 220, F-38043 Grenoble, France

Thomas C. Hansen

Institut Laue Langevin, B. P. 156, F-38042 Grenoble Cedex 9, France

Received April 20, 2000. Revised Manuscript Received June 22, 2000

The crystal structure of the superconducting $K_3Ba_3C_{60}$ fulleride (T_c = 5.4 K) has been studied by synchrotron X-ray and neutron powder diffraction between 10 and 295 K. It is body-centered cubic (bcc) at all temperatures with an essentially half-full t_{1g}-derived band. Close contacts between Ba^{2+} and K^+ ions and neighboring C_{60} units imply a strong orbital hybridization, which leads to broadening of the conduction band. We find that the Ba^{2+} and K^+ cations are disordered in the same distorted tetrahedral interstitial sites, (0, $^1/_2$, $^1/_4 + \delta$), but they are displaced by a different distance (δ) from the center of the site. The resulting local distortions may be responsible for the observed complex relationship between T_c and cubic lattice parameter in $A_3Ba_3C_{60}$ (A = Na, K, Rb, Cs) fullerides.

1. Introduction

Intercalation of solid C_{60} with alkali metals leads to a family of compounds, A_xC_{60} ($1 \le x \le 6$, A = alkali metal) which display a variety of structural, electronic, and magnetic properties.[1] For instance, alkali fullerides with stoichiometry A_3C_{60} are superconducting with critical temperatures (T_c) at ambient pressure as high as 33 K.[2] The superconducting phases adopt, in general, either face-centered-cubic (fcc) or simple cubic structures, in which the three cations occupy the available octahedral and tetrahedral interstitial sites. Charge transfer is essentially complete (with the notable exception of Li and, to a lesser extent, Na fullerides) and the conduction band of C_{60}, which arises from its lowest unoccupied molecular orbital (LUMO) of t_{1u} symmetry is half-filled. T_c scales monotonically with the cubic cell size (a) due to the modulation of the density-of-states at the Fermi level [$N(\epsilon_F)$] by the interfullerene separation.[3] For other stoichiometries and levels of band filling, A_xC_{60} ($x \neq 3$), the superconducting state is suppressed. These compounds adopt a plethora of different crystal structures, showing either insulating or metallic behavior. However, for the latter cases, instabilities, usually of magnetic origin, lead to the occurrence of metal−insulator transitions, precluding the appearance of superconductivity at low temperatures.

Highly doped states of C_{60}^{n-} ($n > 6$) can be synthesized when alkaline earth metals are used as intercalants.[4] In such cases, the conduction band derives from the next unoccupied molecular orbital (LUMO + 1) of C_{60}, which is also triply degenerate with symmetry t_{1g}. Partial occupancy of the t_{1g} orbitals can also lead to certain compositions, which display superconductivity. However, little systematic investigation of the properties of the superconducting members of this fulleride family (AE_xC_{60}) has been undertaken due to the difficulties associated with the synthesis of phase-pure samples. Recent studies have revealed that the behavior of alkaline earth fullerides cannot be directly extrapolated from that of their alkali fulleride antecedents. For example, although Ba_6C_{60} and Sr_6C_{60} are isostructural (space group $Im\bar{3}$) with A_6C_{60} (A = K, Rb, Cs) and should have a nominally full conduction band, they display metallic properties down to low temperatures.[5] In addition, while noncubic A_4C_{60} fullerides are insulating, Ba_4C_{60} and Sr_4C_{60} are bulk superconductors with T_c = 6.7 and 4.4 K, respectively, despite possessing a non-half-filled conduction band and adopting highly aniso-

(1) Prassides, K. *Curr. Opin. Solid State Mater. Sci.* **1997**, *2*, 433. Gunnarsson, O. *Rev. Modern Phys.* **1997**, *69*, 575; Rosseinsky, M. J. *Chem. Mater.* **1998**, *10*, 2665.

(2) Tanigaki, K.; Ebbesen, T. W.; Saito, S.; Mizuki, J.; Tsai, J. S.; Kubo, Y.; Kuroshima, S. *Nature* **1991**, *352*, 222.

(3) Fleming, R. M.; Ramirez, A. P.; Rosseinsky, M. J.; Murphy, D. W.; Haddon, R. C.; Zahurak, S. M.; Makhija, A. V. *Nature* **1991**, *352*, 787.

(4) Kortan, A. R.; Kopylov, N.; Glarum, S.; Gyorgy, E. M.; Ramirez, A. P.; Fleming, R. M.; Zhou, O.; Thiel, F. A.; Trevor, P. L.; Haddon, R. C. *Nature* **1992**, *360*, 566; Baenitz, M.; Heinze, M.; Luders, K.; Werner, H.; Schlogl, R.; Weiden, M.; Sparn, G.; Steglich, F. *Solid State Commun.* **1995**, *96*, 539.

(5) Gogia, B.; Kordatos, K.; Suematsu, H.; Tanigaki, K.; Prassides, K. *Phys. Rev. B* **1998**, *58*, 1077.

10.1021/cm000330i CCC: $19.00
Published on Web 08/25/2000

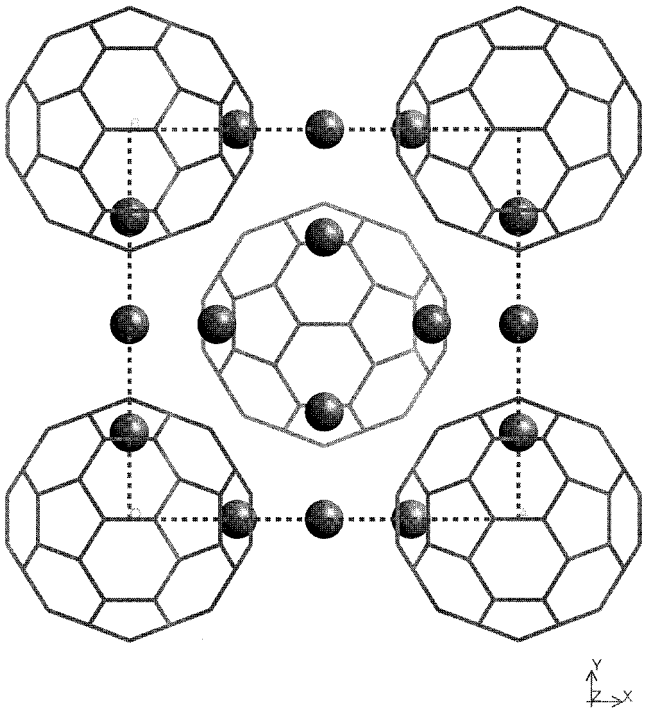

Figure 1. The crystal structure of body-centered cubic $K_3Ba_3C_{60}$. The Ba^{2+} and K^+ ions are shifted from the tetrahedral sites, (0, $^1/_2$, $^1/_4$) to a different extent (δ) but are shown here superimposed for clarity.

tropic orthorhombic structures (space group *Immm*).[6] Such differences between alkali and alkaline earth fullerides, despite their similar or identical structures, have been associated with the effects of hybridization of alkaline earth and C_{60} orbitals (nonrigid band behavior) and the resulting increase in the bandwidth of the t_{1g}-derived band.

Among the alkaline earth salts, the $A_3Ba_3C_{60}$ (A = K, Rb, Cs) family is of particular interest, as the t_{1g} band is formally half-full and the interfullerene separation can be controlled by the size of the alkali cation. Bulk superconductivity is observed for $K_3Ba_3C_{60}$ ($T_c = 5.4$ K) and $Rb_3Ba_3C_{60}$ ($T_c = 2.0$ K), while $Cs_3Ba_3C_{60}$ is not a superconductor down to 0.5 K.[7] Susceptibility measurements show that the density-of-states at the Fermi level, $[N(\epsilon_F)]$ decreases with increasing cell size, in sharp contrast with the A_3C_{60} superconductors. The origin of this behavior is not as yet fully understood, although theoretically it was found that nonrigid band effects should play an important role in determining the superconducting properties.[8] Important information toward this goal may be extracted by detailed structural investigations, as has been the case for Ba_4C_{60},[6] in which a strong interaction between Ba and C_{60}, implying hybridization of Ba 5d and C_{60} t_{1g} orbitals, was revealed. Preliminary structural results have been already reported for $K_3Ba_3C_{60}$, which was shown to adopt a body-centered cubic structure (Figure 1).[7] Due to the similarity in ionic radii of the two cations, the occupation of the interstitial sites by K^+ or Ba^{2+} is random and the structure can be regarded as a 1:1 solid solution of isostructural K_6C_{60} and Ba_6C_{60}.

In an attempt to obtain a better understanding of the structure of $K_3Ba_3C_{60}$ and its implications for superconductivity, we have undertaken a combined high-resolution synchrotron X-ray and neutron diffraction study. By combining the complementary advantages of the two techniques, we have been successful in accurately determining the geometry of the C_{60} cage, the exact composition of the superconducting phase, the local ordering of the two cations in the interstitial sites, and the interaction between the Ba^{2+} and K^+ ions and C_{60}.

2. Experimental Section

The $K_3Ba_3C_{60}$ sample used in the present work was synthesized by intercalation of alkali metals into preformed Ba_3C_{60}.[7] A piece of potassium metal and Ba_3C_{60} powder were loaded in a tantalum cell, sealed under 500 mmHg of helium in a Pyrex tube, and heated at 260 °C for 7 days. Phase purity was confirmed by X-ray diffraction with a Siemens D5000 diffractometer. SQUID measurements were performed on a 47-mg sample sealed in a quartz tube in the temperature range 1.8−30 K with a Quantum Design SQUID magnetometer. Diamagnetic shielding is evident below 5.4 K, signaling the onset of the superconducting transition.

High-resolution synchrotron X-ray diffraction measurements were performed on the $K_3Ba_3C_{60}$ sample sealed in a 0.5-mm diameter glass capillary. Data were collected in continuous scanning mode using nine Ge(111) analyzer crystals on the BM16 beamline at the European Synchrotron Radiation Facility (ESRF, Grenoble, France) at 10 and 295 K ($\lambda = 0.83502$ Å). Data were rebinned in the 2θ range 4°−68° and 4°−58° to a step of 0.01° at 10 and 295 K, respectively. Analysis of the diffraction data at both temperatures was performed with the GSAS suite of Rietveld analysis programs.[9]

Additional temperature-dependent synchrotron X-ray diffraction measurements on the same sample were also performed on the Swiss-Norwegian beamline (BM1A) at the ESRF with a 300-mm diameter Mar Research circular image plate. A monochromatic X-ray beam of $\lambda = 0.88095$ Å and dimensions 0.5×0.5 mm^2 was focused onto the sample by sagittal bending of the second crystal of a double-crystal Si(111) monochromator. The sample was cooled from 320 to 105 K at a rate of 25 K/h. Cooling was by means of an Oxford Cryosystems Cryostream cold nitrogen blower. Images of the Debye−Sherrer rings were measured every 5 min with a sample to detector distance of 200 mm and with an exposure time of 40 s. One-dimensional diffraction patterns were obtained by integrating around the rings using local software (program FIT2D). Data analysis was performed with the Fullprof suite of Rietveld analysis programs.[10]

The neutron diffraction experiment on $K_3Ba_3C_{60}$ was undertaken with the high-flux high-resolution diffractometer D2b ($\lambda = 1.5944$ Å) at the Institute Laue Langevin, Grenoble, France. The sample (0.58 g) from the same batch used for synchrotron X-ray measurements was loaded in a cylindrical vanadium can (diameter = 5 mm) sealed with indium wire and then placed in a standard ILL "orange" liquid helium cryostat. The instrument was operated in its high-resolution mode (10′ horizontal primary divergence, 1 cm horizontal monochromator aperture), and the data were collected in the angular range $2\theta = 0°-164.5°$ in steps of 0.05°. A full diffraction profile was measured with counting time of 10 h

(6) Brown, C. M.; Taga, S.; Gogia, B.; Kordatos, K.; Margadonna, S.; Prassides, K.; Iwasa, Y.; Tanigaki, K.; Fitch, A. N.; Pattison, P. *Phys. Rev. Lett.* **1999**, *83*, 2258.

(7) Iwasa, Y.; Hayashi, H.; Furudate, T.; Mitani, T. *Phys. Rev. B* **1996**, *54*, 14960; Iwasa, Y.; Kawaguchi, M.; Iwasaki, H.; Mitani, T.; Wada, N.; Hasegawa, T. *Phys. Rev. B* **1998**, *57*, 13395.

(8) Umemoto, K.; Saiti, S.; Oshiyama, A. *Phys. Rev. B* **1999**, 60, 16186.

(9) Larsen, A. C.; von Dreele, R. B. GSAS software, Los Alamos National Laboratory Report No. LAUR 86-748.

(10) Rodriguez-Carvajal, J. *Program Fullprof* (version 3.5, Dec 97), ILL (unpublished).

at 10 K. The raw data were merged, while applying angular and efficiency (vanadium) detector calibrations, using standard ILL programs. The data analysis was performed with the GSAS software.[9]

3. Results

The synchrotron X-ray and neutron powder diffraction profiles at 10 K did not show any reflections violating body centered cubic (bcc) extinction rules, thus implying the absence of any structural transitions with the crystal structure of $K_3Ba_3C_{60}$ remaining bcc to low temperatures. A combined Rietveld refinement of the two data sets was attempted in space group $Im\bar{3}$, previously employed in the structural determinations of bcc fulleride salts.[11] In the starting structural model, the C_{60} units, modeled as undistorted truncated icosahedral units with $R = 3.57$ Å, were placed at the origin of the unit cell and were orientationally ordered with their 2-fold symmetry axes aligned along the cube edges. The K^+ and Ba^{2+} cations, each with fixed fractional occupancy $n = {}^1/_2$, were disordered over the same distorted 12e tetrahedral sites (0, ${}^1/_2$, ${}^1/_4 + \delta$; $\delta \approx 0.03$). Refinement proceeded smoothly with this model which, however, only gave moderate agreement with the data (combined agreement factors: $R_{wp} = 8.6\%$; $R_{exp} = 5.8\%$).[12] Various possibilities were then systematically explored in the refinement. First, both the K^+ and Ba^{2+} ions were allowed to move independently within the tetrahedral interstices by relaxing the constraint on their positional parameters. This led to different displacements from the tetrahedral site, $\delta = 0.0343(20)$ and $\delta = 0.0265(8)$ for K^+ and Ba^{2+}, respectively. Following improvement of the refinement, the fractional occupancies of the two cations were also allowed to vary subject to the constraint, $n_K + n_{Ba} = 1$. The values obtained were $n_K = 0.512(8)$ and $n_{Ba} = 0.484(8)$ and imply only a marginally small excess of potassium. Finally, the stability of the combined Rietveld refinement of the profiles was not affected even when the C_{60} positional parameters were varied unconstrained. The results of the final refinement at 10 K are shown in Figure 2 [$R_{wp} = 7.5$, $R_{exp} = 5.8\%$; $a = 11.21661(7)$ Å] with the fitted parameters summarized in Table 1.

The high-resolution synchrotron X-ray data on $K_3Ba_3C_{60}$ collected at room temperature were also refined using the structural model obtained from the combined Rietveld refinement at low temperature. The refinement proceeded routinely, leading to a cubic lattice constant, $a = 11.2433(2)$ Å ($R_{wp} = 11.8\%$, $R_{exp} = 9.2\%$). Synchrotron X-ray powder diffraction profiles were also collected on slow cooling from 320 to 105 K. Extraction of reliable lattice constants down to 150 K was performed using sequential Rietveld analysis in the 2θ range 1°−34° (at 320 K, lattice constant $a = 11.2460(3)$ Å; agreement factors $R_{wp} = 9.7\%$, $R_{exp} = 2.7\%$). The temperature dependence of the lattice constant of $K_3Ba_3C_{60}$ is shown in Figure 3. The linear thermal expansivity, α ($\equiv$d ln a/dT), is calculated to be equal to $9.54(2) \times 10^{-6}$ K^{-1} between 320 and 105 K. The small value of α is consistent with the much tighter crystal packing in $K_3Ba_3C_{60}$ (cf. $\alpha = 2.20(6) \times 10^{-5}$ K^{-1} for Na_2CsC_{60} and $2.02(3) \times 10^{-5}$ K^{-1} for Li_2CsC_{60} in the same temperature range).[14]

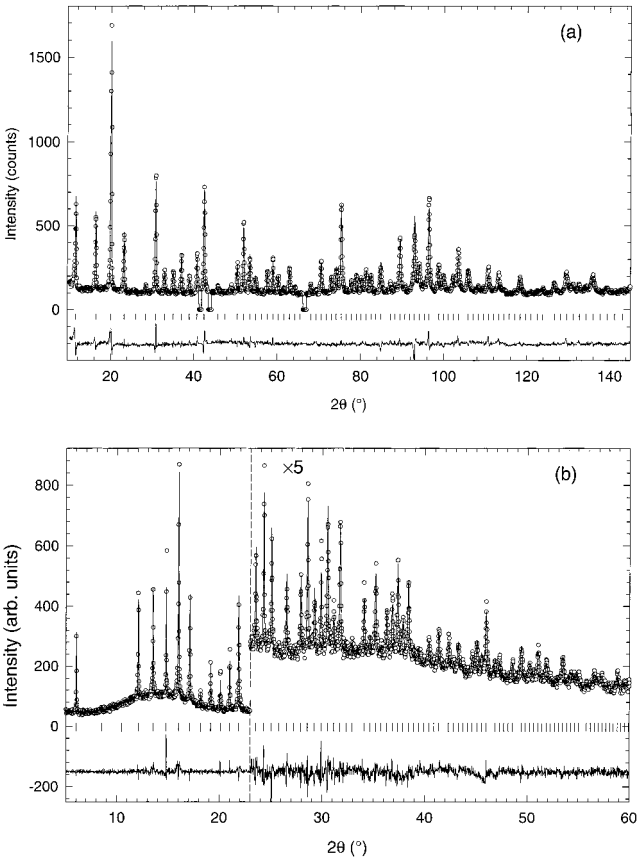

Figure 2. Final observed (○) and calculated (solid line) powder (a) neutron ($\lambda = 1.5944$ Å) and (b) synchrotron X-ray ($\lambda = 0.83502$ Å) diffraction profiles for $K_3Ba_3C_{60}$ at 10 K. In each case, the lower solid line shows the difference profile and the tick marks show the reflection positions. The profile in b has been expanded for clarity by a factor of 5 at Bragg angles larger than 23°.

Table 1. Refined Atomic Parameters for $K_3Ba_3C_{60}$ Obtained from Combined Rietveld Refinement of Synchrotron X-ray and Neutron Powder Diffraction Data at 10 K[a]

atom	site	x	y	z	B (Å^2)	n
K	12e	0	0.5	0.2843(20)	0.72(6)	0.512(8)
Ba	12e	0	0.5	0.2765(8)	0.72(6)	0.484(8)
C(3)	24g	0.06407(2)	0	0.31118(8)	0.51(2)	1.0
C(4)	48h	0.12792(3)	0.10360(3)	0.27151(7)	0.51(2)	1.0
C(5)	48h	0.06407(2)	0.20736(5)	0.23303(6)	0.51(2)	1.0

[a] Space group, $Im\bar{3}$; combined reliability factors, $R_{wp} = 7.5\%$, $R_{Exp} = 5.8\%$; synchrotron X-ray data, $R_{wp} = 6.6\%$; neutron data, $R_{wp} = 7.8\%$. The cubic cell constant ls $a = 11.21661(7)$ Å.

(11) Zhou, O.; Fischer, J. E.; Coustel, N.; Kycia, S.; Zhu, Q.; McGhie, A. R.; Romanow, W. J.; McCauley, J. P.; Smith, A. B.; Cox, D. E. *Nature* **1991**, *351*, 462.

(12) Inspection of the high-resolution synchrotron X-ray diffraction profiles collected on the BM16 diffractometer shows that the peaks display pronounced asymmetry which arises from axial divergence. In general, a pseudo-Voigt function is employed routinely in Rietveld refinement procedures to describe the observed reflection peak shape. In the present case, use of the asymmetry function of Finger et al.[13] was found to improve the refinement considerably. This involves two additional refinable parameters, S/L and H/L, which model the peak asymmetry. L is the distance between sample and detector, $2S$ is the size of the illuminated sample, and $2H$ is the aperture of the detector slit. The S/L and H/L parameters were refined at the early stages and were subsequently fixed to values $S/L = 6.2 \times 10^{-3}$ and $H/L = 5.0 \times 10^{-4}$.

(13) Finger, L. W.; Cox, D. E.; Jephcoat, A. P. *J. Appl. Crystallogr.* **1994**, *27*, 892.

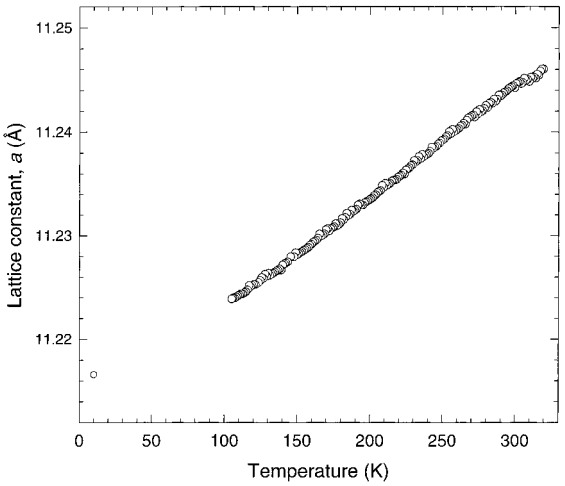

Figure 3. Temperature dependence of the cubic lattice constant (a) of $K_3Ba_3C_{60}$ obtained on cooling.

4. Discussion

A perspective view of the coordination environment of both Ba^{2+} and K^+ ions is shown in Figure 4. Each ion occupies distinct distorted tetrahedral sites with different coordination environments with the C_{60} units—facing two hexagonal and two pentagonal faces of four neighboring C_{60} units—and shifted from each other by 0.088(9) Å. This is consistent with the presence of substantial anisotropies in the reorientational potential of the C_{60} units, observed by neutron inelastic scattering.[15] The values of the average C−M distances [3.261(4) Å and 3.259(9) Å for Ba^{2+} and K^+, respectively] are identical due to the almost equal ionic radii of the two cations (1.35 and 1.33 Å for Ba^{2+} and K^+, respectively). Evidence for hybridization between the 5d orbitals of Ba and the 2p orbitals of carbon is provided by the value of the shortest Ba−C distance [Ba−C(5) = 3.0849(8) Å, Table 2], which is only marginally larger than the sum of the van der Waals C radius (1.70 Å) and the Ba^{2+} ionic radius. This implies the same strong orbital mixing observed in Ba_4C_{60}, in which short Ba−C contacts of 2.983(3) and 3.044(6) Å were identified,[7] even though the extent of the interaction is somewhat weaker in $K_3Ba_3C_{60}$. However, it is important to note that the K−C contact is also short [K−C(5)= 3.0809(9) Å, Table 2] compared to other K^+-containing fullerides, thus also suggesting hybridization between the C_{60} and K states. Our structural results are in good agreement with the findings of LDA calculations[8] of the electronic structure of $K_3Ba_3C_{60}$, in which hybridization between C_{60} and Ba and K states was found to result in a broad conduction band. However, the theoretical calculations do not include any of the anisotropy effects arising from the distinct occupation of the tetrahedral sites by Ba^{2+} and K^+, identified in the present work. Such effects may further modify sensitively the details of the electronic structure and the conduction band in the $K_3Ba_3C_{60}$ superconductor, which is much broader with a lower

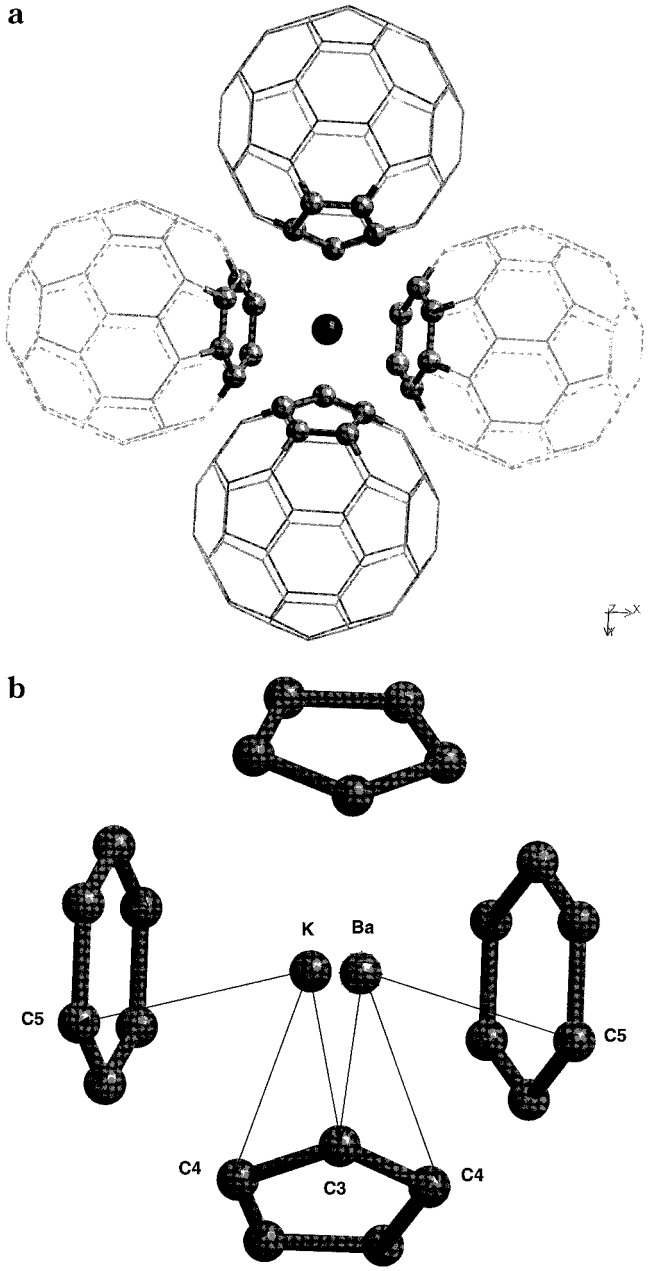

Figure 4. (a) Perspective view of the tetrahedral interstice in the bcc structure of $K_3Ba_3C_{60}$. (b) Coordination environment of the Ba^{2+} and K^+ ions to two pentagonal and two hexagonal faces of the neighboring C_{60}^{9-} ions. The shift between the two cations has been amplified for clarity.

$N(\epsilon_F)$ (11.4 states eV^{-1} (mol $C_{60})^{-1}$)[7] than those in the t_{1u} superconductors, despite the similar band filling.

Further indication of the existence of orbital mixing was obtained by the determination of the C_{60}^{9-} cage geometry. In the $Im\bar{3}$ space group, three different carbon atoms are needed to describe the fulleride unit (Table 1). The results of the combined Rietveld refinement show that the C_{60}^{9-} units in $K_3Ba_3C_{60}$ are essentially undistorted. The three nonequivalent C atoms are at similar distances from the center of the molecule [$R_{C(3)}$ = 3.564(4) Å, $R_{C(4)}$ = 3.561(9) Å, $R_{C(5)}$ = 3.5718(9) Å], implying that the C_{60}^{9-} cage is well-described as a sphere of radius R = 3.566(5) Å. A tendency for a small outward deviation from sphericity is only observed for C(5), which lies slightly above the surface of the sphere,

(14) Margadonna, S.; Brown, C. M.; Lappas, A.; Prassides, K.; Tanigaki, K.; Knudsen, K. D.; Le Bihan, T.; Mézouar, M. *J. Solid State Chem.* **1999**, *145*, 471. Margadonna, S.; Brown, C. M.; Prassides, K.; Fitch, A. N.; Knudsen, K. D.; Le Bihan, T.; Mézouar, M.; Hirosawa, I.; Tanigaki, K. *Int. J. Inorg. Mater.* **1999**, *1*, 157.

(15) Margadonna, S.; Li, W. Z.; Prassides, K.; Neumann, D. A. *Chem. Phys. Lett.* **2000**, *322*, 472.

Table 2. Selected Carbon−Carbon and Metal−Carbon Distances (Å) in $K_3Ba_3C_{60}$ at 10 K

6:6 bonds	C(3)−C(3)	1.4372(4) (×6)	Ba−C(3)	3.188(7) (×2)	K−C(3)	3.254(17) (×2)
	C(4)−C(5)	1.4331(3) (×24)		3.360(7) (×4)		3.294(17) (×4)
mean 6:6 bond		1.4339(3)	Ba−C(4)	3.231(4) (×4)	K−C(4)	3.195(9) (×4)
6:5 bonds	C(3)−C(4)	1.4357(4) (×24)		3.270(5) (×4)		3.316(12) (×4)
	C(4)−C(5)	1.4506(4) (×24)	Ba−C(5)	3.0849(8) (×4)	K−C(5)	3.0809(9) (×4)
	C(5)−C(5)	1.4372(5) (×12)		3.395(1) (×4)		3.409(4) (×4)
mean 6:5 bond		1.4420(4)	mean Ba−C	3.261(4)	mean K−C	3.259(9)

possibly manifesting its interaction with Ba^{2+} and K^+ ions.

The combined Rietveld refinement was also designed to investigate the geometry of the C_{60}^{9-} anion as the high reduction state could sensitively affect the cage dimensions. In general, it has been anticipated theoretically that the fullerene cage will expand and the bond length alternation found in pristine C_{60} [d(6:6) = 1.391(8) Å, d(6:5) = 1.455(8) Å] will gradually smooth out with increased reduction state.[16] This arises from the gradual population of the t_{1u} levels, which are predominantly bonding at the 6:5 and antibonding at the 6:6 C−C bonds. The trends have been confirmed experimentally up to a reduction state of −6 (K_6C_{60}) for which the average 6:6 and 6:5 bond distances are essentially equal [1.445(3) and 1.432(10) Å, respectively] and the radius of C_{60}^{6-} has increased to 3.560(4) Å.[17] Further increase of the nominal charge to −9 in $K_3Ba_3C_{60}$ is achieved by populating the t_{1g} orbitals, which are of similar character to t_{1u}. The observed bond alternation appears negligible [d(6:5) − d(6:6) = 0.0081(7) Å, Table 2], in agreement with theoretical estimates for C_{60}^{12-} on the order of 0.01 Å,[16] while the radius of C_{60}^{9-} is 3.566(5) Å.

Finally, independent refinement of the fractional occupancies of K and Ba has allowed the determination of the superconducting composition as $K_{3.07(5)}Ba_{2.90(5)}C_{60}$. Naive electron count indicates that the effective formal charge of C_{60} is −8.88(14) for this composition, and within the error bars the t_{1g}-derived band is nominally half-full, in sharp contrast with the less than half-full band of superconducting Ba_4C_{60}.

5. Conclusions

Combined neutron and synchrotron X-ray powder diffraction measurements were employed to study in detail the structure of superconducting $K_3Ba_3C_{60}$, which adopts a bcc structure at all temperatures. The structural analysis revealed the positional disorder of the Ba^{2+} and K^+ ions in the distorted tetrahedral sites and the existence of short Ba−C and K−C contacts, implying strong hybridization between the K, Ba, and C_{60} states. In addition, refinement of the fractional occupancies of K and Ba indicates that in the superconducting phase the t_{1g} band is essentially half-full. The orbital mixing strongly modifies the shape of the conduction band, leading to a larger bandwidth and a smaller value of $N(\epsilon_F)$ than those encountered in t_{1u} superconductors, despite the similar band filling.

The complex relationship between the lattice parameter and T_c in the bcc $A_3Ba_3C_{60}$ superconductors (A = K, Rb, and their mixtures)—$K_3Ba_3C_{60}$ has a higher T_c than $Rb_3Ba_3C_{60}$, although the latter has a larger lattice constant—may also arise as a result of such orbital mixing. Unemoto et al.[8] attempted to explain this discrepancy in terms of the presence of an isotope effect with the mass difference between K and Rb leading to the observed anomaly in T_c. On the basis of this isotope-effect mechanism, $Na_3Ba_3C_{60}$ should show a higher T_c than $K_3Ba_3C_{60}$, as a result of the smaller mass of Na^+. However, we recently synthesized $Na_3Ba_3C_{60}$, which turned out not to become superconducting down to 2 K.[18] Thus T_c is maximized for $K_3Ba_3C_{60}$ and decreases for both smaller and larger lattice constants. Attempts to explain this novel trend may be quite premature at present, as accurate structure determinations are not available for $Na_3Ba_3C_{60}$ and $Rb_3Ba_3C_{60}$. Nevertheless, we note that in $K_3Ba_3C_{60}$ there is a perfect matching between the size of K^+ and Ba^{2+} ions, while in both the Rb^+ and Na^+ analogues there exists a considerable mismatch. This is expected to have important structural and electronic consequences. For instance, the occupied site difference between Rb^+ and Na^+ and divalent Ba^{2+} should be even more pronounced than the one established for $K_3Ba_3C_{60}$, leading to increased local distortions and anisotropies and, consequently, reduced T_c.

Acknowledgment. We thank the NEDO Frontier Carbon Technology program and the Royal Society for financial support, the European Synchrotron Radiation Facility (ESRF) and the Institut Laue Langevin (ILL) for provision of synchrotron X-ray and neutron beamtime, respectively and Dr Ken Knudsen for help with the BM1 experiment.

CM000330I

(16) Andreoni, W.; Giannozzi, P.; Parrinello, M. *Phys. Rev. B* **1995**, *51*, 2087.

(17) Allen, K. M.; David, W. I. F.; Fox, J. M.; Ibberson, R. M.; Rosseinsky, M. J. *Chem. Mater.* **1995**, *7*, 764.

(18) Margadonna, S.; Aslanis, E.; Prassides, K. Unpublished results.